Design and Analysis of Venturi Microbubble Generator Using Computational Fluid Dynamics

Thoharudin*[1], Sunardi [2], Fitroh Anugrah Kusuma Yudha[3], Muhammad Nadjib[4], Arif Setyo Nugroho[5]

[1,2,3,4]*Department of Mechanical Engineeing, Universitas Muhammadiyah Yogyakarta, Indonesia*

[5]*Department of Mechanical Engineeing, Sekolah Tinggi Teknologi Warga, Indonesia*
*Email address: **thoharudin@ft.umy.ac.id***

Abstract— **The necessity for dissolved oxygen in water is crucial for the survival and growth of aquatic organisms, particularly tilapia. Seventy-five percent of tilapia will die if there is insufficient dissolved oxygen in the water. This work seeks to develop a venturi bubble-generating technique to combat the scarcity of dissolved oxygen in the water. A floating pump with a capacity of 12 m³/hour was selected as the medium for distributing water and generating vacuum pressure to draw in air for mixing with the water flow in the venturi. Ansys Fluent was used to model piping and venturi systems. The piping system was modeled with a single-phase (water) flow at a steady state, whereas the flow in the venturi was modeled with a multiphase (air and water) flow under transient situations. The simulation findings revealed that the pressure drop at the 90-degree elbow was much greater (27.17 kPa) than that at the 45-degree elbow (16.53 kPa). A 1-inch input diameter venturi produced bubbles with an average diameter of 105 μm, whereas a ½ inch venturi bubble generator produced bubbles with an average diameter of 83 μm. Owing to the numerous advantages of adopting a six-outlet piping system with a ½ inch venturi, this design is recommended for floating pumps with a capacity of 12 m³/h.**

Keywords—Aerator, CFD Simulation, Microbubble generator, Venturi.

I. INTRODUCTION

The concentration of dissolved oxygen (DO) in water is essential for the survival and growth of aquatic organisms, particularly Tilapia (Oreochromis niloticus). Reducing the concentration of dissolved oxygen in the water (hypoxia) is detrimental to Tilapia's survival, development, and immune system [1]. Typically, Tilapia requires 6.0–6.5 mg/L of dissolved oxygen in the water [2].

At night, when photosynthesis is not taking place, stagnant water is more likely to have hypoxic conditions than moving water because currents and convection do not supply dissolved oxygen (DO) into these bodies of water. Although while fish can utilize a variety of different methods to adjust for decreased DO uptake, this can have an influence on their overall health and susceptibility to bacterial infections, particularly Aeromonas hydrophila, which is the pathogen that kills many different species of fish. In addition, hypoxia slows the growth of fish by reducing their ability to absorb nutrients from their food. As a direct consequence of this, the average size and weight of the fish that are taken will be lower [3].

This hypoxic issue also happens in tilapia ponds, particularly in reservoirs where fish rely only on natural water circulation to receive enough dissolved oxygen. The fish mortality rate in ponds is between 50 and 75 percent. Preserving water quality in aquaculture is essential for maximizing fishing yield. Aeration is a standard technique for maintaining water quality [4]. In semi-intensive and intensive aquaculture, aeration systems are crucial for maintaining an environment consistent with the physiological needs of the organisms being cultivated by dispersing airborne particles that allow oxygen transport to the water. Aeration delivers oxygen to aquatic species so they can consume dissolved oxygen from water and remain alive [5]. The most common aeration systems used in aquaculture are gravity, surface, diffuser, turbine aerators, spiral aerators, propeller vacuum pump aerators, stepped cascade aerators, including circular stepped waterfall aerators, clustered circular stepped waterfall aerators and several other types, including microbubble (MB) systems, and nanobubble (NB) aerations [6].

MB and NB systems refer to bubbles having 1–100 m and 1 m diameters, respectively (ISO 20480-1, 2017). In the case of macro bubbles with a large diameter, buoyancy plays a crucial role in determining the bubble's ascent rate towards the water's surface. It is noted that 5–6 meters per minute is the observed vertical velocity of macro bubbles [7]. Due to their diminutive size, micro and nano bubbles act differently than macro bubbles [8]. Unlike macro bubbles, which rise rapidly to the surface of water, MB tend to shrink, rise slowly (because having poor buoyancy), and dissolve into the surrounding water. A 10 μm in diameter MB has a vertical velocity of 3 mm/min [9]. Meanwhile, NB can remain stable in water for weeks or months, as long as viscosity, buoyancy, and bubble weight are in static equilibrium [10], [11]. Through MB-type aeration, the dissolved oxygen content in water can increase up to 36.06% [12]. A venturi bubble generator is the simple technology for producing MB [13], [14].

The structure of the venturi bubble generator consists of three main components: the convergent section, throat, and diverging section. The working principle of the venturi is based on Bernoulli's energy conservation principle. As liquid flows through the venturi passages, velocity (kinetic energy) increases in the throat, accompanied by a decrease in pressure (pressure energy). The pressure drop in the throat section can draw in ambient air until it mixes with the water flow. In the diverging section, the inserted air bubbles fragment into finely dispersed bubbles (NB and MB) in the water stream [15]. The smaller the size of the air bubbles increases the diffusivity of oxygen into the water.

The objective of this project is to design an aerator system utilizing venturi microbubble generator technology to combat hypoxia in tilapia ponds. The piping system was designed to reduce energy loss due to pressure drop and the venturi bubble generator was designed and analyzed using Ansys Fluent software to predict the size of the air bubbles created by the venturi bubble generator.

49

II. METHODS

The design of the aerator system was intended for a pond with dimensions of 11 m x 17 m with a capacity of 6000 tilapia fish. This design was divided into two parts, namely, the piping system design and the venturi bubble generator design, where the two designs used Ansys Fluent software. Simulations for the piping system and the venturi bubble generator were made in three dimensions to achieve high accuracy. The piping system was simulated with a single phase (water) at a steady state. The k−ε turbulence model was chosen because it has good accuracy for various flow models. Pressure and speed were coupled through the SIMPLE scheme to accelerate convergence in the iteration process. Momentum, turbulent kinetic energy, and turbulent

dissipation rate were discretized by the second-order upwind method, while pressure was calculated by the PRESTO method.

The diameter of a 1-inch PVC pipe was chosen to meet the outlet pipe diameter of the floating pump with a capacity of 12 m3/hour. A comparison was made between two piping system designs: one with three outlets (1-inch venturi bubble generator) and one with six outlets (half-inch diameter venturi bubble generator). Fig. 1a and b illustrate the simulated piping system. Around the border of the pond, a piping system with three outlets was constructed, while a piping system with six outlets was constructed across the middle pond. In a six-outlet piping system, the pipe outlets were connected to 1 inch to ½ inch reducers.

a

b
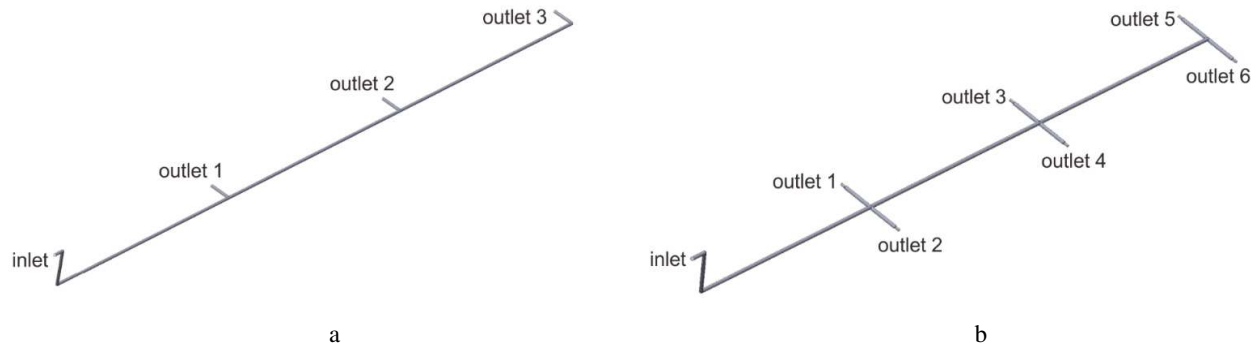
Fig. 1. Aerator piping system design: a) three outlets, b) six outlets.

Unlike the piping system design, which involves a single phase, the venturi bubble generator involves two phases: liquid and gas. Therefore, the multiphase Eulerian-Eulerian transient model was implemented in this simulation. The population balance model was performed to illustrate the process of aggregation and separation of air bubbles. The air bubble aggregation rate was calculated using the Luo model [16] and the Lehr model simulated the separation rate [17]. The k−ω turbulence model, SST, was used because it has unique advantages in predicting flow separation and behavior in pressure gradients [18]. Pressure and speed are connected via a SIMPLE phase couple scheme; momentum, turbulent

kinetic energy, specific dissipation rate, and water bin are discretized using the second-order upwind method; pressure is calculated by the PRESTO method; and the volume fraction was estimated by the QUICK method.

The simulated venturi bubble generator had a diameter of 1 inch and ½ inch, with the same inlet and outlet angles, namely 30º, while the diameter of the air inlet was 2 mm, based on literature [13], [14]. The designed throat diameter was fifty percent of the pipe diameter, and the total length of both types of venturi bubble generators, 100 mm, was identical. Fig. 2a and b depict illustrative examples of a venturi bubble generator.

a

b
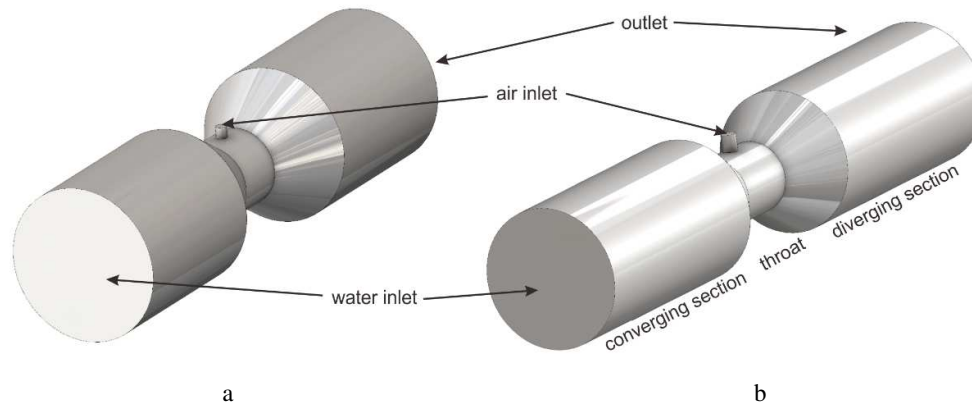
Fig. 2. Design of a venturi bubble generator: a) 1 inch, b) ½ inch

III. RESULTS AND DISCUSSION

A. Design of Piping System

The elbow fitting is necessary for determining the pressure drop in the pipe flow. This elbow fitting was used to direct water to a depth of 0.5 meters below the water's surface

in order to dissolve the air drawn into the venturi bubble generator into the water body. The 90-degree elbow profile was compared to the 45-degree elbow profile to see which one performed better, as shown by the lower pressure drop. During water flow at a depth of 0.5 m below the water's surface, a 45-degree elbow profile necessitated a longer pipe channel. Even

50

though the 90º elbow profile having a shorter pipeline, it showed a substantially larger pressure drop than the 45º elbow profile (Fig. 3).

Using the 90º and 45º elbow profiles, the pressure drop in the pipe flow was 27,2 kPa and 16,5 kPa, respectively.

Although requiring a longer pipeline, the 45º elbow profile produced a pressure drop that was about half that of the 90º elbow profile. Thus, a piping system with a 45-degree elbow design was chosen to transport water to a depth of 0.5 meters below the water's surface.

a   b
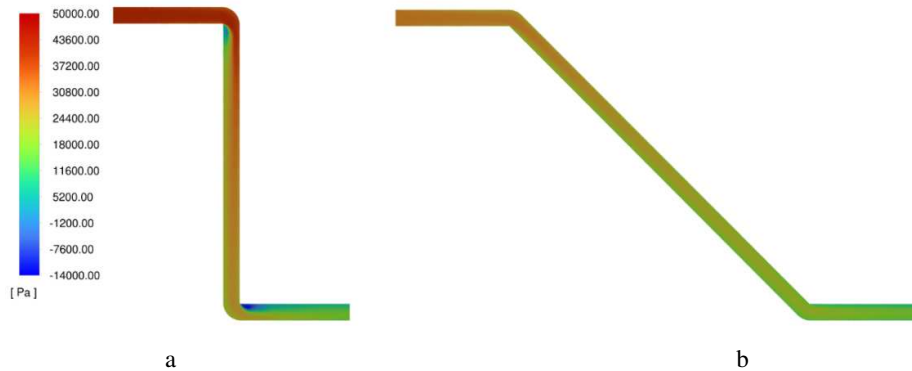
Fig. 3. Pressure contours of the piping system with the elbow profile of: a) 90-degree, b) 45-degree

Fig. 4a and b depict the pressure contours on the piping system for both three outlet channels and six outlets. Despite the presence of a reducer from 1 inch to ½ inch diameter pipes in the system, a piping system with six outlets requires a lower intake pressure (66.15 kPa) than a system with three outlets (87.82 kPa) to move 12 m³/hr of water. On the six outlet channel, the piping system needed to be as long as 8.25 m (horizontally in the middle of the pond, 0.5 m below the water surface), whereas on the three outlet channel, it required a channel that was 12.75 m longer (horizontally along the edge of the pond, 0.5 m below the water surface).

a   b
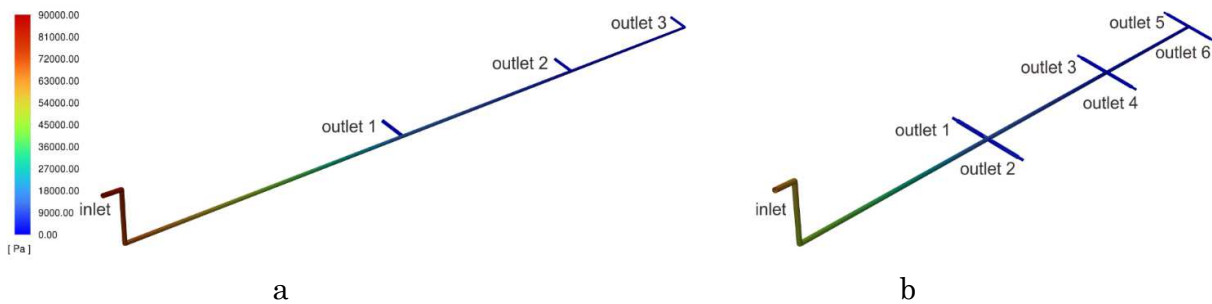
Fig. 4. Pressure contours of the piping system with: a) three outlets, b) six outlets

Table 1 displays a comparison of the flow characteristics of the three-outlet and six-outlet piping systems. In general, the pressure and flowrate varied and tended to decrease with increasing distance from the intake in both the three- and six-outlet piping systems. The water that is pushed often exits through an outlet that is near to the inlet. In a three-outlet piping system, as much as 54.05 percent of water exited from outlet 1, and on a six-outlet piping system, as much as 46.16 percent of water exited from outlets 1 and 2. Moreover, the pressure drop between the intake and each outlet in the three outlet piping system was larger than that of the six outlet system. Hence, the power loss on the flow with the three-outlet piping system was assessed to be 278.15 watts, which was more than the power loss on the flow with the six-outlet piping system, which was 208.51 watts. To equalize the flow rate at each outlet, valves must be installed at outlets 1 and 2 in the three-outlet piping system and at outlets 1 to 4 in the six-outlet piping system.

TABLE 1. COMPARISON OF FLOW CHARACTERISTICS OF THREE OUTLET AND SIX OUTLET PIPING SYSTEMS

Parameter	Pressure (kPa)	Water Flowrate (Liter/minute)
Piping system with thee-outlet		
Inlet	87.82	196.27
Outlet 1	4.44	106.08
Outlet 2	1.09	52.72
Outlet 3	0.54	37.47
Piping system with six-outlet		
Inlet	66.15	196.27
Outlet 1	3.71	45.16
Outlet 2	3.75	45.43
Outlet 3	1.38	27.55
Outlet 4	1.38	27.58
Outlet 5	1.16	25.21
Outlet 6	1.17	25.33

B. Design of Venturi Bubble Generator

By adding valves, the outlet flow discharge could be equalized in both three-outlet and six-outlet piping systems, resulting in a uniform outlet flow velocity. In a piping system with three outlets, each outlet had a flow rate of 65.42 liters per minute. With a 1 inch outlet diameter, the outflow velocity

51

was 1.8 meters per second. In the six-outlet piping system, the discharge for each outlet was 32.71 liters per minute, and the flow velocity was 1.95 meters per second using a ½ inch outlet pipe diameter.

To measure the velocity of incoming air in the venturi bubble generator, the experimental study performed by Sakamatapan et al. [14] was employed to find out the correlation between water and air discharge. The intake air flowrate of the venturi bubble generator was positively correlated with the inlet water debit. Figure 5 depicts the relationship between the input velocities of water and air derived from the correlation. Utilizing these data, it was determined that the inlet air velocity in the system with three outlets and a water intake speed of 1.8 m/s was 0.0156 m/s, while the inlet air velocity in the system with six outlets and a water inlet speed of 1.95 m/s was 0.0184 m/s.
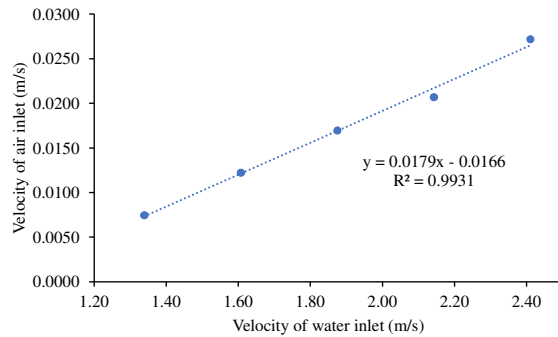
Figure 5. The relationship between inlet water velocity and inlet air velocity

Fig. 6 depicts the velocity profile of the water flow through the venturi bubble generator, with the highest velocity achieved in the throat region. In accordance with Bernaulli's Law, as the velocity in the throat region increased, so did the pressure generate in that region (Fig. 10). When traveling through the throat region, the water velocity tended to be high, faster than before entering the throat region. This is a result of the difference in the cross-sectional area of the channel, which is smaller in the throat region. In addition, the entry of air into the venturi flow caused a rise in fluid volume, such that the volume of fluid after entering the throat area consisted of collected water and air and produced a high velocity. In the 1 inch venturi bubble generator, water velocity was segregated and tended to flow in the lower region, however in the ½ inch venturi bubble generator, water velocity was more evenly distributed. This is impacted by the influx of air, which halts the movement of water in the throat region (Fig. 8). Due to the low kinetic energy of the low water velocity in the 1 inch venturi bubble generator, the water flow direction is easily disrupted when air flows in from multiple directions. Due to the larger kinetic energy of water flow, the water velocity in the ½ inch venturi bubble generator tended to be more homogeneous and equally distributed across the venturi.
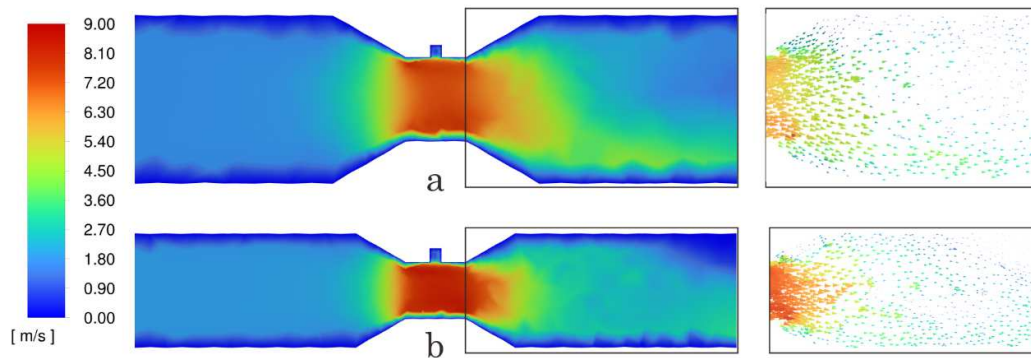
The phenomena of more uniform velocity distribution in the ½ inch venturi bubble generator was also influenced by high turbulence, where the turbulence level of the ½ inch venturi bubble generator was greater and more uniform than that of the 1 inch venturi bubble generator (Fig. 7). High turbulence promoted more uniform mixing of air and water, resulting in a more homogeneous flow velocity.

The ratio of the standard deviation of the flow fluctuations to the average flow velocity is the definition of turbulence intensity, which represents the intensity of the flow velocity fluctuations. Clearly, the high turbulence strength was only observed when the water and air mixed. This shows that the air entering the throat caused a region of intense turbulence, reaching about 100 percent.

Figure 6. Contour of air velocity in the venturi bubble generator: a) 1 inch, b) ½ inch
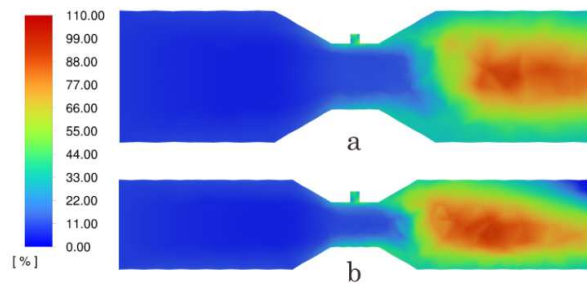
Fig. 7. Contour of turbulence intensity in the venturi bubble generator: a) 1 inch, b) ½ inch

Fig. 8 depicts the air velocity profile in the venturi bubble generator. In the 1 inch venturi bubble generator, the air velocity tended to alter the direction of the water flow velocity, whereas this effect was minimal in the ½ inch venturi bubble generator. The mixing of air and water was significantly influenced by the rate of water flow in the neck region (Fig. 6). Due to the high-water velocity in the neck region, water and air were better mixed. Hence, flow separation did not occur in the ½ inch venturi bubble generator, as its flow velocity at the throat area was greater than that of the 1 inch venturi bubble generator.
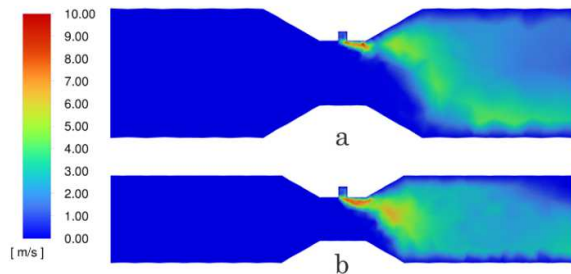
Fig. 8. Contour of air velocity in the venturi bubble generator: a) 1 inch, b) ½ inch

Fig. 9 depicts the distribution of bubble diameters in a venturi bubble generator. The bubble dimensions and distributions produced by a 1 inch venturi bubble generator are comparable to those produced by a ½ inch venturi bubble generator. When air entered through the air inlet channel, the bubbles that form tended to have a big diameter. Nevertheless, because to the rapid mixing with water, the bubbles divided and became small/fine. The 1 inch venturi bubble generator produced bubbles with an average diameter of 105 m, while the ½ inch size generated bubbles with an average diameter of 83 µm. Lee et al. [13] discovered an average bubble size of 50 to 250 µm based on the entry and exit angles of the venturi, whereas Sakamatapan et al. [14] observed bubbles with a diameter of 100 to 130 µm based on the water flow rate.
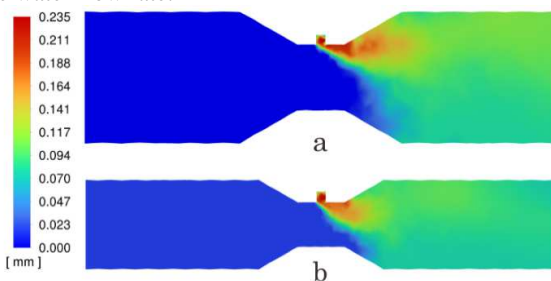
Fig. 9. Contour of bubble diameter distributed in the venturi bubble generator: a) 1 inch, b) ½ inch

In the venturi bubble generator, the pressure decreased significantly from the entrance to the throat region (converging section). The pressure then raised marginally in the region following the throat (diverging section). The throat's low pressure served to draw air from the atmosphere into the venturi bubble generator. On a 1 inch venturi bubble generator, the average input and output pressure difference was 13.42 kPa, while it was 16.47 kPa on a ½ inch venturi bubble generator. The 1 inch venturi bubble generator had a mass flow rate of water of 1.09 kg/s, resulting in a power loss of 14.63 watts; the 12 inch venturi bubble generator had a mass flow rate of water of 0.54 kg/s, resulting in a power loss of 8.98 watts. The 1 inch venturi bubble generator had a total power loss of 43.89 watts after the installation of a three outlet piping system. 53.89 watts of power were lost in the ½ inch venturi bubble generator installation (a piping system with six outlets).
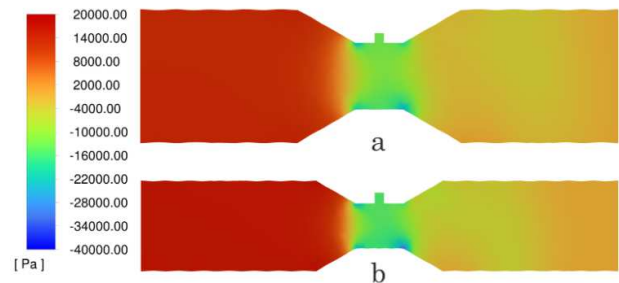
Fig. 10. Contour of presssure in the venturi bubble generator: a) 1 inch, b) ½ inch

The air inlet diameter of 1 inch and ½ inch Venturi bubble generators was the same, at 2 mm. With a velocity of 0.015 m/s and 0.018 m/s, the mass flow rate of incoming air was 3.61 mg/minute and 4.24 mg/minute, respectively. A 1-inch venturi bubble generator was installed on a piping system with three outlet channels, while a ½-inch venturi bubble generator was installed on a piping system with six outlets. Consequently, the total inlet air mass flow rate for the three-outlet piping system was 10.82 mg/min, whereas the inlet air mass flow rate for the six-outlet piping system was 25.47 mg/min.

IV. CONCLUSIONS

Using the Ansys Fluent program, the venturi bubble generator was designed and analyzed. Using a floating pump with a capacity of 12 m³/hour, water was pumped via a 1 inch PVC pipe. The 45-degree elbow pipe arrangement was selected due to its smaller pressure drop. The piping system was built with two different outlet configurations: three and six. Due to the difference in installation location, the three outlet piping system requires a longer pipe line than the six outlet piping system. In order to achieve a comparable venturi bubble generator inlet velocity, the venturi inlet diameter in the three-outlet piping system was the same as the pipe diameter, but in the six-outlet piping system it was half the diameter (½ inch). The simulation showed that the three outlet piping system created greater power loss than the six outlet system due to the longer piping channel.

The performance of the ½ inch Venturi bubble generator was superior to that of the 1 inch size. This was demonstrated by uniform water and air velocities, smaller/finer bubble diameters, and a higher overall air mass flow rate. Although having a greater overall power loss (53.89 watts), the ½ inch venturi bubble generator had a superior oxygen distribution in

53

the pond in terms of bubble size, number of outlet channels, and air mass flow rate. Featuring six outlet channels, the ½ inch venturi bubble generator will produce more uniformly distributed bubbles in the pond. The amount of air injected into water using a ½ inch venturi bubble generator will expedite the increase in dissolved oxygen concentration. Also, the ½ inch venturi bubble generator was installed on a six outlet piping system, which had a smaller power loss than a three outlet channel due to the shorter length of the piping. Thus, a piping system with six outputs and a ½ inch venturi bubble generator is suggested for applications using a venturi-type aerator with a discharge capacity of ½ m³/hour.

REFERENCES

[1] V. A. Prakoso and Y. J. Chang, "Pengaruh Hipoksia terhadap Konsumsi Oksigen pada Benih Ikan Nila (Oreochromis niloticus)," *Oseanologi dan Limnol. di Indones.*, vol. 3, pp. 165–171, 2018, doi: 10.14203/oldi.2018.v3i2.169.

[2] M. Abdel-Tawwab, A. E. Hagras, H. A. M. Elbaghdady, and M. N. Monier, "Effects of dissolved oxygen and fish size on Nile tilapia, Oreochromis niloticus (L.): growth performance, wholebody composition, and innate immunity," *Aquacult Int*, vol. 23, pp. 1261–1274, 2015, doi: 10.1007/s10499-015-9882-y.

[3] F. A. Huntingford *et al.*, "Coping strategies in a strongly schooling fish, the common carp Cyprinus carpio," *J. Fish Biol.*, vol. 76, pp. 1576–1591, 2010, doi: 10.1111/j.1095-8649.2010.02582.x.

[4] I. Prasetyaningsari, A. Setiawan, and A. A. Setiawan, "Design optimization of solar powered aeration system for fish pond in Sleman Regency, Yogyakarta by HOMER software," *Energy Procedia*, vol. 32, pp. 90–98, 2013, doi: 10.1016/j.egypro.2013.05.012.

[5] S. Zhou, M. Liu, B. Chen, L. Sun, and H. Lu, "Microbubble- and nanobubble-aeration for upgrading conventional activated sludge process: A review," *Bioresour. Technol.*, vol. 362, p. 127826, 2022, doi: 10.1016/j.biortech.2022.127826.

[6] E. De Oro Ochoa, M. Carmona García, N. Durango Padilla, and A. Martínez Remolina, "Design and experimental evaluation of a Venturi and Venturi-Vortex microbubble aeration system," *Heliyon*, vol. 8, p. e11096, 2022, doi: 10.1016/j.heliyon.2022.e11096.

[7] A. Agarwal, W. J. Ng, and Y. Liu, "Principle and applications of microbubble and nanobubble technology for water treatment," *Chemosphere*, vol. 84, no. 9, pp. 1175–1180, Aug. 2011, doi: 10.1016/j.chemosphere.2011.05.054.

[8] M. Liu, T. Li, Z. Wang, T. Radu, H. Jiang, and L. Wang, "Effect of aeration on water quality and sediment humus in rural black-odorous water," *J. Environ. Manage.*, vol. 320, p. 115867, 2022, doi: 10.1016/j.jenvman.2022.115867.

[9] A. Endo *et al.*, "DO-increasing effects of a microscopic bubble generating system in a fish farm," *Mar. Pollut. Bull.*, vol. 57, pp. 78–85, 2008, doi: 10.1016/j.marpolbul.2007.10.014.

[10] B. Choi, T.-Y. Jeong, and S. Lee, "Application of jetventurimixer for developing low-energy-demand and highly efficient aeration process of wastewater treatment," *Heliyon*, vol. 8, p. e11096, 2022, doi: 10.1016/j.heliyon.2022.e11096.

[11] A. Basso, F. A. Hamad, and P. Ganesan, "Effects of the geometrical configuration of air–water mixer on the size and distribution of microbubbles in aeration systems," *Asia-Pacific J. Chem. Eng.*, vol. 13, pp. 1–11, 2018, doi: 10.1002/apj.2259.

[12] M. Wu, S. Yuan, H. Song, and X. Li, "Micro-nano bubbles production using a swirling-type venturi bubble generator," *Chem. Eng. Process. - Process Intensif.*, vol. 170, p. 108697, 2022, doi: 10.1016/j.cep.2021.108697.

[13] C. H. Lee, H. Choi, D.-W. Jerng, D. E. Kim, S. Wongwises, and H. S. Ahn, "Experimental investigation of microbubble generation in the venturi nozzle," *Int. J. Heat Mass Transf.*, vol. 136, pp. 1127–1138, 2019, doi: 10.1016/j.ijheatmasstransfer.2019.03.040.

[14] K. Sakamatapan, M. Mesgarpour, O. Mahian, H. S. Ahn, and S. Wongwises, "Experimental investigation of the microbubble generation using a venturi-type bubble generator," *Case Stud. Therm. Eng.*, vol. 27, p. 101238, 2021, doi: 10.1016/j.csite.2021.101238.

[15] J. Huang *et al.*, "A review on bubble generation and transportation in Venturi-type bubble generators," *Exp. Comput. Multiph. Flow*, vol. 2, pp. 123–134, 2020, doi: 10.1007/s42757-022-0132-z.

[16] H. Luo and H. F. Svendsen, "Theoretical model for drop and bubble breakup in turbulent dispersions," *AIChE J.*, vol. 42, pp. 1225–1233, 1996, doi: 10.1002/aic.690420505.

[17] F. Lehr, M. Millies, and D. Mewes, "Bubble-Size distributions and flow fields in bubble columns," *AIChE J.*, vol. 48, pp. 2426–2442, 2002, doi: 10.1002/aic.690481103.

[18] N. Dutta, P. Kopparthi, A. K. Mukherjee, N. Nirmalkar, and G. Boczkaj, "Novel strategies to enhance hydrodynamic cavitation in a circular venturi using RANS numerical simulations," *Water Res.*, vol. 204, p. 117559, 2021, doi: 10.1016/j.watres.2021.117559.